Applied Surface Science 258 (2012) 7889–7896

Contents lists available at SciVerse ScienceDirect

Applied Surface Science

journal homepage: www.elsevier.com/locate/apsusc

Physico-chemical characterization of functionalized polypropylenic fibers for prosthetic applications

Roberto Nisticò[a], Maria Giulia Faga[b,*], Giovanna Gautier[b], Giuliana Magnacca[a], Domenico D'Angelo[c], Emanuele Ciancio[c], Giacomo Piacenza[c], Roberta Lamberti[d], Selanna Martorana[d]

[a] Department of Chemistry and NIS Center of Excellence, University of Torino, Via P. Giuria 7, Torino 10125, Italy
[b] CNR-ISTEC, Strada delle Cacce 73, Torino 10135, Italy
[c] Clean-NT Lab, Environment Park S.P.A., Via Livorno 60, 10144 Turin, Italy
[d] Herniamesh S.r.l., Via F.lli Meliga, 1/C 10034 Chivasso, Turin, Italy

ARTICLE INFO

Article history:
Received 27 January 2012
Received in revised form 12 April 2012
Accepted 17 April 2012
Available online 9 May 2012

Keywords:
Hernia
Fiber
Polypropylene
Chitosan deposition
Activating plasma treatment

ABSTRACT

Polypropylene (PP) fibers can be manufactured to form nets which can find application as prosthesis in hernioplasty.

One of the most important problem to deal with when nets are applied in vivo consists in the reproduction of bacteria within the net fibers intersections. This occurs right after the application of the prosthesis, and causes infections, thus it is fundamental to remove bacteria in the very early stage of the nets application.

This paper deals with the physico-chemical characterization of such nets, pre-treated by atmospheric pressure plasma dielectric barrier discharge apparatus (APP-DBD) and functionalized with an antibiotic drug such as chitosan.

The physico-chemical characterization of sterilized nets, before and after the functionalization with chitosan, was carried out by means of scanning electron microscopy (SEM) coupled with EDS spectroscopy, FTIR spectroscopy, drop shape analysis (DSA), X-ray diffraction and thermal analyses (TGA and DSC).

The aim of the work is to individuate a good strategy to characterize this kind of materials, to understand the effects of polypropylene pre-treatment on functionalization efficiency, to follow the materials ageing in order to study the effects of the surface treatment for in vivo applications.

1. Introduction

Infections in hernioplasty may have different sources, one above all the choice of prosthetic mesh [1–5]. Polypropylene (PP) is one of the most widely used polymers in the world and is the most common surgical non-absorbable mesh used in hernioplasty, urologic and gynecologic surgery [6,7].

PP standard-weight meshes (70–140 g/m^2), firstly used, are often substituted by the light-weight ones (35–70 g/m^2), more comfortable for the patient because made up of thinner filament that guarantee an increase of prosthesis flexibility [8]. New generations of biomaterials used in hernioplasty are lightweight implants often associated with a network of absorbable material in order to progressively reduce the prosthesis weight favoring the new cellular tissues growth.

Before being implanted in vivo, prosthetic biomaterials need necessarily to be sterilized to avoid the infections onset. The sterilization technique chosen for this work is the treatment with ethylene oxide because it involves ambient temperature treatments producing a lower surface oxidation than high energy radiations [9–11].

The discussion around the strategy of prevention and post-surgery treatment of infections is still open. In this respect, the aim of this work is the characterization of a novel surgical mesh with antibiotic properties in order to prevent infections directly in the surgical site.

This is achieved by combining an antibiotic bioresorbable polymer with lightweight polypropylene mesh.

Chitosan is a very cheap polymer obtained by N-deacetylation of chitin and commercially available primarily from the shellfish industry's waste [12]. This natural polymer has become of great interest as a new functional biomaterial of high potential in various fields because of its excellent biological properties such as non-toxicity, biocompatibility and biodegradability. It is commonly used in the biomedical field as carrier for biological active species,

* Corresponding author. Tel.: +39 011 3977616; fax: +39 011 346288.
E-mail address: m.faga@to.istec.cnr.it (M.G. Faga).

0169-4332/$ – see front matter © 2012 Elsevier B.V. All rights reserved.
http://dx.doi.org/10.1016/j.apsusc.2012.04.113

because of its capability to coordinate transition metals. Moreover, chitosan possesses its own antimicrobial activity to many Gram-positive bacteria (e.g. *Staphylococcus aureus*) and Gram-negative bacteria (e.g. *Pseudomonas aeruginosa* and *Escherichia coli*) [1]. The exact mechanism of chitosan antimicrobial activity is not yet fully known, even if some hypothesis have been formulated in literature [2].

S. aureus (which is the most common bacterial infection cause) has a medium diameter of about 1 μm, thus it may infiltrate all surgical meshes, while macrophages (the cells of our body whose function is to phagocytate bacteria) have a higher diameter comparing to the pores of surgical meshes and cannot prevent bacteria infiltration. Therefore, the local prevention of bacterial colonization is required. A possible strategy to perform this action is to cover PP meshes with a chitosan layer which can directly act against bacteria.

Interactions between chitosan and polypropylene surface is guaranteed by a controlled oxidation process of the fibers surface carried out by an atmospheric pressure plasma (APP-DBD) in oxidizing atmosphere device through which it is possible to functionalize the polypropylene surface generating species capable to form hydrogen bonds (hydroperoxides, alcohols, carboxylic acids) with the chitosan polar groups [13–19].

2. Experimental

2.1. Materials

Sterilized polypropylene (PP in the following) meshes from Herniamesh® S.r.l. (Chivasso, Italy).

Meshes ready for functionalization with antibiotic component were previously treated by Clean NT Lab in a APP-DBD plasma apparatus fed with the oxidizing mixture on each net side.

Polypropylene film for food packaging was used for comparison purposes: it will be indicated as REF in the text.

Chitosan, *medium molecular weight* by *Aldrich*, CAS 9012-76-4. It was prepared in acetic acid/water solution following the procedure described in [15]. The final concentration of chitosan was 2.4% w/v where the solvent is 2% v/v of glacial acetic acid in water. Glacial acetic acid was from *Aldrich*, 99.7% of purity, CAS 64-19-7.

Physiological solution (0.9% NaCl w/v in water) by B. Braun, Italia.

Spackman reactive for ninhydrin test was prepared as described in [20]: it was used to obtain a quantitative determination of chitosan.

2.2. Methods

Bioactive film deposition on implants was carried out immediately after plasma treatment of the surgical meshes and consists in soaking the net in a crystallizer containing the chitosan solution. Subsequently, the excess of chitosan solution is removed from the meshes by a simple drip and the bioactive film is dried at ambient temperature for 24 h.

Scanning electron microscopy (SEM) analyses were carried out using a ZEISS EVO 50 XVP with LaB_6 source, equipped with detectors for secondary electrons collection and EDS probe for elemental analyses. Samples are insulating, thus they were covered with a gold layer of ~15 nm of thickness before the analysis to avoid any charging effect (Bal-tec SCD050 *sputter coater*). The presence of gold in EDS spectra (principal signal at ~2.2 keV) is due to this step and will not be evidenced in the following data discussion.

FTIR spectra were recorded in both transmission and attenuated total reflection mode (diamond cell for single reflection) in a Bruker IFS28 spectrophotometer equipped with Globar source, DTGS detector and working with 128 scans at 4 cm^{-1} of resolution in the range 4000–400 cm^{-1}. FTIR analysis in transmission was carried out on KBr diluted pellets of chopped fibers; ATR spectra were obtained on single fibers repeating the acquisition for three times.

Sample preparation for FTIR spectroscopy deserves some consideration. The analysis of meshes in transmission mode resulted very difficult because of their very sparse texture: the IR radiation does not interact enough with samples to allow good spectra collection. For this reason we decided to prepare pellets in KBr using the mesh finely chopped, with the aim to concentrate the sample in a transparent medium to obtain good signals. This way, it was possible to obtain good IR absorptions. For proving the method, some ATR-FTIR spectra were carried out on a single fiber. It was possible to confirm the results obtained by transmission spectra. Nevertheless, the use of ATR cell resulted more complex because the alignment of sample in the diamond cell required more than one measurement in order to avoid artifacts or false signals. For this reason, we decided to present all the FTIR spectra collected in transmission mode, although a lot of them were obtained following both the procedures.

Drop shape analysis (DSA) was performed by using a Kruss DSA 100 with 25× optical zoom available. The analysis was done with a drop of 3 μl of double distilled water and with a released drop rate of 600 μl/min. The instrument automatically calculates the contact angle (repeated three times), that indicates the hydrophilicity/hydrophobicity ratio of the material surface.

X-ray diffraction patterns were obtained using the diffractometer PW3040/60 X'Pert PRO MPD from PANalytical, in Bragg-Brentano geometry, equipped with the high power ceramic tube PW3373/10 LFF source with Cu anode.

Thermal analyses were carried out by means of TGA Q600 and DSC Q200 by TA Instruments.

For TGA analyses, the experimental program used is the following: $T = 40\,^{\circ}C$ for 1 min in nitrogen, ramp of 10 °C/min up to 800 °C in nitrogen, $T = 800\,^{\circ}C$ for 10 min in air (to eliminate all the organic residue).

For DSC analyses, completely carried out in nitrogen, the experimental program used is the following: $T = 40\,^{\circ}C$ for 1 min, ramp of 20 °C/min up to 190 °C, ramp of 10 °C/min down to 40 °C, $T = 40\,^{\circ}C$ for 1 min; ramp of 20 °C/min up to 190 °C. The successive repetition of the same heating cycle allows to evidence the presence of some not-reproducible phenomenon.

The phase transition peak area compared with the calorimetric constant determined for an appropriate standard material allows to obtain the phase transition enthalpy. In this case we observed melting (heating cycle) and crystallization (cooling cycle) of PP.

The crystallinity degree of polymer (X_{cr}) is determined comparing $\Delta_m H$ obtained for polymer and $\Delta_m H^*$ tabled for completely crystalline, isotactic polypropylene (209 J/g [9]), following the equation $(\%\, X_{cr}) = \Delta_m H / \Delta_m H^* \times 100$.

Colorimetric quantification of chitosan was performed using a UV-mini-1240 by Shimadzu. All the spectra were obtained using a plastic cuvette, 20 scans per spectrum with a scan time of 30 s. 0.5 ml of chitosan solution and 0.5 ml of ninhydrin solution were mixed by hand in a covered test tube and dipped immediately for 30 min in a boiling water bath (at this stage the primary amino group reacts with ninhydrin forming a purple solution). The tube was then cooled by immersion in a cold water bath and the tube contents was diluted in a beaker containing 2 ml of a solution of ethanol/water 50% v/v, shacking vigorously for 30 s to oxidize the excess of hydridantin [21]. Colorimetric spectra were obtained repeating the acquisition for two times.

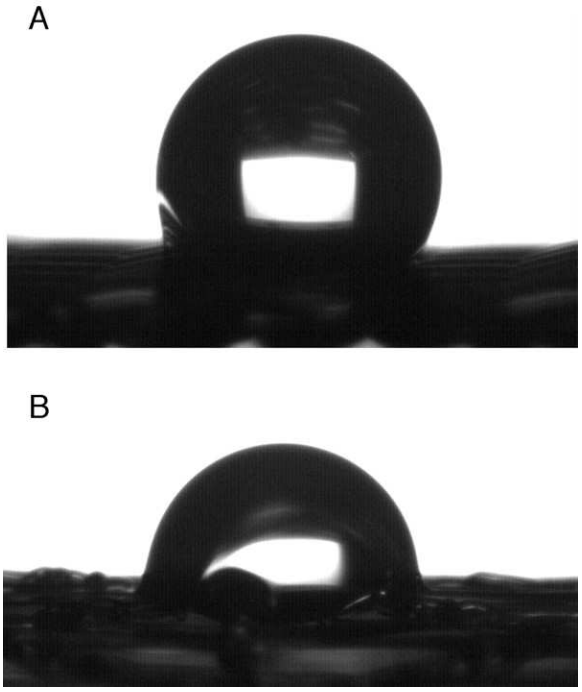

Fig. 1. DSA observed for PP fibers before plasma treatment (A) and after plasma treatment (B).

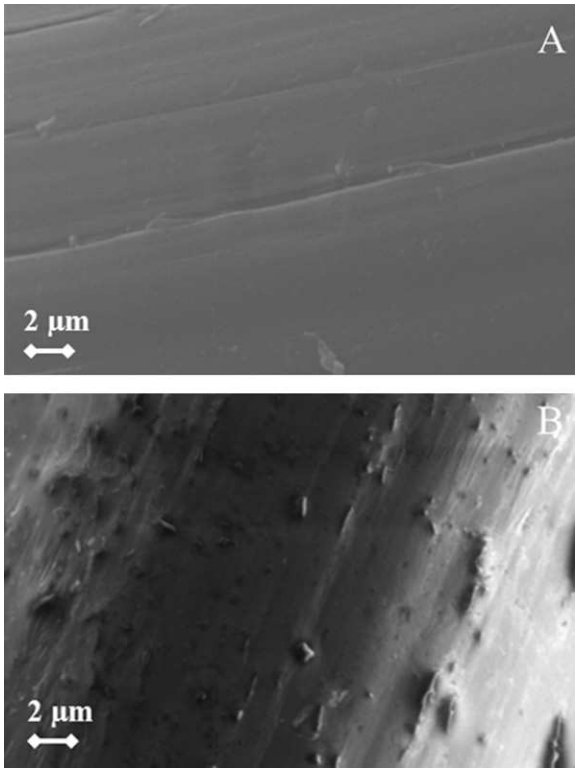

Fig. 2. SEM images of sterilized fibers before (A) and after (B) the oxidizing plasma treatment.

3. Results and discussion

3.1. Sterilized PP fibers before and after oxidizing plasma treatments

The oxidation of the polypropylenic fibers is fundamental to make them more hydrophilic, so that interactions between chitosan polar group and polypropylene meshes become possible. The contact between the mesh and chitosan solution can be studied with DSA tests where water simulates the aqueous chitosan solution. DSA images of the polypropylene surface before and after the plasma treatment (Fig. 1) explain the plasma effect on the surface modification and the subsequent hydrophilicity developed by PP fibers. Images show that the water–solid contact angle passes from $132.0^\circ \pm 0.4$ for untreated fiber, to $98.5^\circ \pm 1.8$ for plasma treated sample. This indicates that untreated nets present an accentuated apolarity that should avoid the chitosan layer formation, whereas the plasma treatment increases the hydrophilicity of the fibers giving a better contact with aqueous solutions.

SEM images of some PP sterilized fibers before and after the oxidizing plasma treatments are reported in Fig. 2. Before the treatment (Fig. 2A), the fibers appear almost regular in size, smooth on the surface, with some shallow incisions along the fiber length.

EDS analyses indicate the presence of carbon, as expected for polypropylene (spectra omitted for sake of brevity).

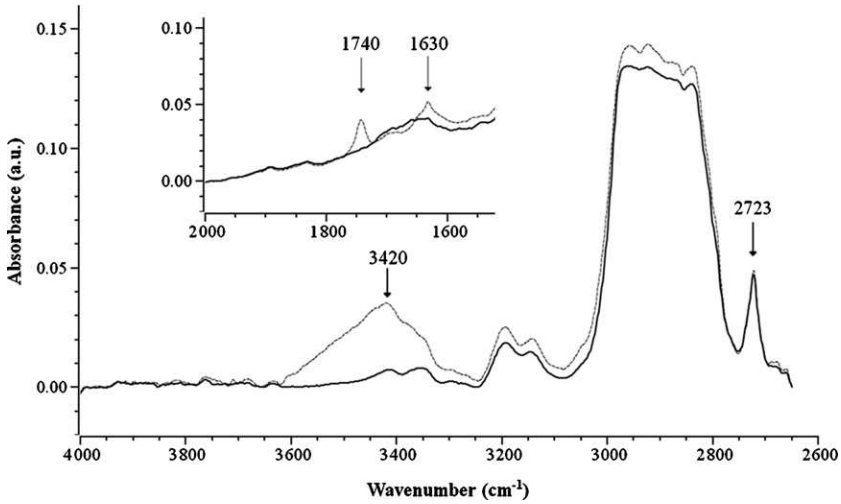

Fig. 3. Absorbance FTIR spectra in the 4000–2600 cm^{-1} range collected in transmission mode: PP fibers dispersed in KBr before (solid line) and after (dashed line) plasma treatment. The spectra were normalized on the intensity of PP signals at 2723 cm^{-1} in order to evidence the 3420 cm^{-1} signal growth. In the inset the same spectra in the range 2000–1400 cm^{-1} are reported, in order to evaluate the presence of carbonylic groups absorption at 1740 cm^{-1}.

Table 1
DSC data for polypropylene fibers before and after plasma treatment compared with reference film results.

Sample	No. of measures	T_c (°C) ± Dev. Std.	T_m (°C) ± Dev. Std.	$\Delta_m H$ (J/g) ± Dev. Std.	X_{cr} (%) ± Dev. Std.
PP fibers (before plasma treatment)	3	112.9 ± 0.5	168.0 ± 1.5	102.8 ± 4.6	49 ± 2
PP fibers (after plasma treatment)	3	113.4 ± 0.4	173.8 ± 2.0	125.8 ± 2.9	60 ± 1
REF film	3	112.7 ± 0.8	160.1 ± 0.7	72.1 ± 3.4	34 ± 2

After the plasma treatment (Fig. 2B), the fibers appear wrinkled, the surface being much more irregular, indicating that also a mechanical interaction can occur with polymeric film.

Fig. 3 shows the absorbance FTIR spectra of fibers dispersed in KBr before and after the plasma treatment.

The most important signals are due to polypropylene chains in the range 3000–2800 cm^{-1} (ν_{CH}). Oxidizing plasma treatment causes the formation of a broad band extending from 3600 down to 3300 cm^{-1} due to surface hydroperoxides and alcohols involved in hydrogen bonds [9–11]. However, since water signals can disturb this absorbance band, also the peaks ranging between 1800 and 1600 cm^{-1} (Fig. 3, inset) are reported. It can be observed the enhancement of water signal intensity at ~1630 cm^{-1} (δ_{HOH}) as a consequence of the plasma treatment, indicating that also the contribution of water in the hydroperoxides signals need to be taken into account. Otherwise, atmospheric pressure plasma also forms esters, ketones and/or carboxylic acids on polypropylene surface, as witnessed by the appearance of the bands at 1740 cm^{-1} due to carbonylic groups [11]. The presence of both carbonylic groups and hydroperoxides signals confirms the oxidation of the material carried out by plasma treatment.

XRD measurements (not shown) carried out on PP samples before and after the plasma treatment do not evidence any difference caused by plasma oxidation. In fact, only signals due to isotactic polypropylene, α phase, are present in both cases [22,23].

DSC measurements allowed to evaluate the crystallinity degree of PP mesh in comparison with a PP film taken as a reference material.

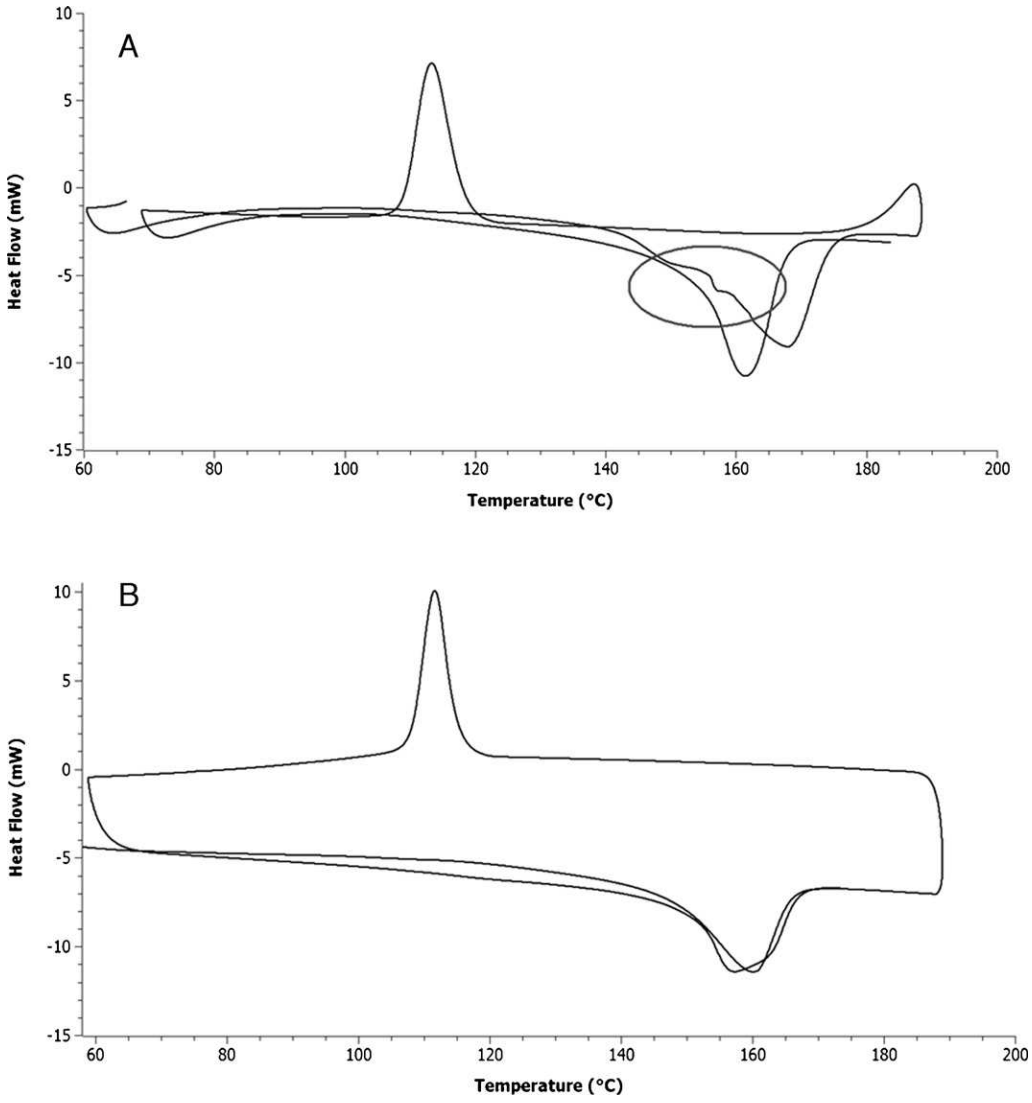

Fig. 4. DSC curves observed for PP fibers before plasma treatment under heating–cooling–second heating process in inert atmosphere of nitrogen (A) and DSC curves observed for the reference film under heating–cooling–second heating process in inert atmosphere of nitrogen (B). The circle drawn in top section evidences the broadening of melting range.

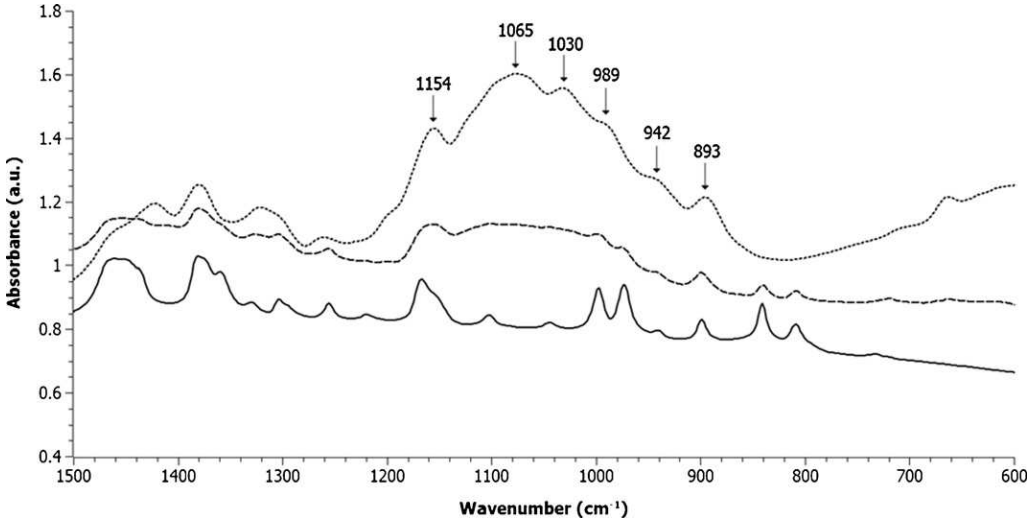

Fig. 5. Absorbance FTIR spectra in the 1500–600 cm^{-1} of polypropylene fiber plasma treated (solid line), chitosan powder (dotted line) and polypropylene fiber functionalized with chitosan film (dashed line). All the spectra were obtained in transmission mode.

Similar curves are collected for PP sample before and after plasma treatment: only data obtained for PP before plasma treatment are reported for the sake of brevity, and the main relevant data of all analyzed samples are summarized in Table 1.

The first heating cycle carried out on PP sample before plasma treatment is reported in Fig. 4 (top section) and evidences the presence of many shoulders above the melting peak causing the broadening of the melting range. This may be due to two circumstances: the presence of a biphasic system (for instance, an α phase and a β phase that melt at different temperatures, generating a shoulder on the main endothermic peak) or a non-perfect adherence of the sample at the bottom of the aluminum sample holder (the first melting of the fibers next to the heated surface is followed by the progressive melting of the others, so that the melting range become wider than normal).

XRD analysis of the same sample does not evidence the presence of a second crystalline phase (only α phase monoclinic reflections are visible in the relative diffractogram), moreover the second heating cycle shows only one endothermic peak indicating that the observed phenomenon is not reversible. This suggests that the reason of this odd behavior is the not-perfect adhesion of the sample at the heating holder: after the first heating, the molten fibers form a film on the bottom of the sample holder and the second heating occurs normally. However, the comparison between the enthalpies obtained from both cycles, did not give consistent differences. For this reason, only the results obtained for the first heating cycle were considered.

Despite these limitations, the temperatures determined for the melting process and reported in Table 1 are comparable with those reported in the literature [23]. Moreover, melting temperatures determined for the nets are very similar to those determined for the reference sample.

The most interesting application of DSC technique, from our point of view, consists in the determination of PP fibers crystallinity degree (X_{cr}). Applying the equation already mentioned in Section 2.2, we obtained the average value of $X_{cr} = 49 \pm 2\%$ for PP fibers before plasma treatment, absolutely similar to that reported for commercial fibers. Reference film sample shows a crystallinity degree of $X_{cr} = 34 \pm 2\%$, very similar to that of commercial films (usually less crystalline than fibers). Unexpectedly, PP fibers after plasma treatment shows a crystallinity degree of $X_{cr} = 60 \pm 1\%$: this quite high value (about 10% higher than PP fibers before plasma

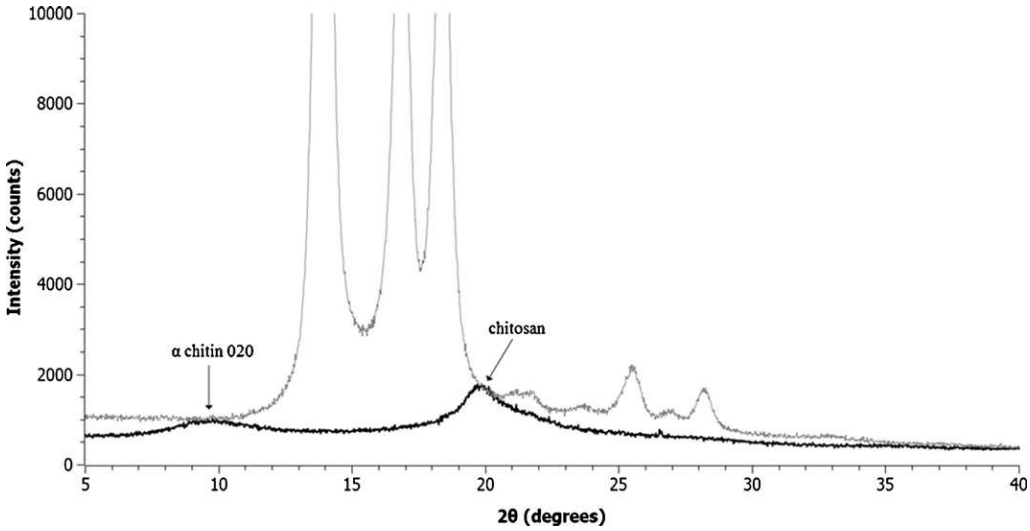

Fig. 6. XRD curve of PP fibers after chitosan deposition (gray line) compared with the main patterns of chitosan powder (black line).

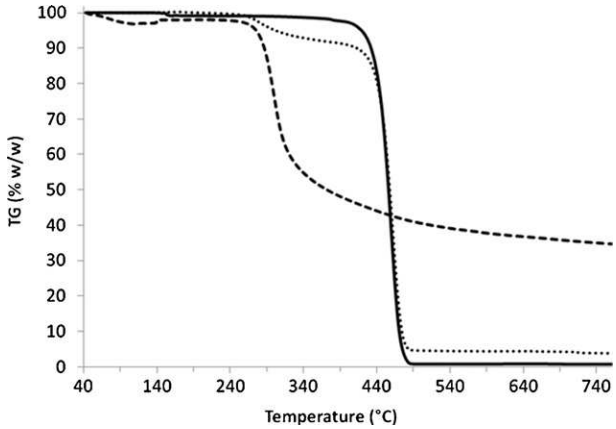

Fig. 7. TG curves of PP fibers (solid line), chitosan in powder (dashed line) and PP fibers functionalized with chitosan (dotted line) obtained from a heating process in inert atmosphere of nitrogen.

treatment) is probably caused by UV radiation generated by glow-discharge during plasma treatment [24].

3.2. Plasma treated PP fibers after chitosan deposition

Chitosan film adhesion is evaluated after immersion of meshes in physiological solution.

The FTIR spectra of plasma treated fibers before and after chitosan deposition is reported in Fig. 5, together with the spectrum of chitosan powder. The presence of a wide band centered at $\sim$1050 cm^{-1} is certainly due to chitosan, since its main absorptions (see the spectrum of chitosan powder) falls in the range 1150–890 cm^{-1} [25].

XRD carried out on PP fibers after chitosan deposition reveals only the presence of signals due to isotactic polypropylene α phase (Fig. 6). No signals due to chitosan or to the chitosan precursor (chitin) are visible, indicating that the presence of chitosan deposited on PP fibers cannot be determined by XRD [26].

TG analysis allows to observe the presence of chitosan deposited on treated prosthetic meshes. Fig. 7 reports the gravimetric curves for PP meshes, chitosan powder and PP fibers after chitosan deposition. PP meshes show a small oscillation of the weight loss at the melting point of the polymer (T_m = 168.0 ± 1.5 °C), and the PP degradation in the temperature range from 415 to 490 °C with the maximum degradation rate at T_{mdr} = 455 °C. Polypropylene is almost completely degraded in inert atmosphere (nitrogen), leaving a residue at 800 °C of about 0.7% w/w [27]. Chitosan powder shows a first weight change at low temperatures due to water loss; after that, an important weight decrease starts at 285 °C and continues up to the end of the heating, leaving a residue of $\sim$35% w/w. The chitosan degradation brings about amino groups and hydrogen loss with formation of graphitic-like unsaturated system [28–30]. Finally, PP fibers functionalized with chitosan show two degradation steps, the first one given by chitosan modification occurring in the range 285–415 °C, and the latter due to PP degradation in the range 415–490 °C. In this case, a residue of $\sim$3.6% w/w is left. Being neglectable the residue due to PP material, the amount of residue left by functionalized nets allows to quantify the amount of chitosan deposed on PP fibers, corresponding to $\sim$10% w/w.

The chitosan adhesion to PP fibers was evaluated to understand if the chitosan deposition procedure is functional and effective and if the functionalized material is actually suitable for in vivo application. This test is carried out by soaking the functionalized mesh (6 cm × 11 cm) in physiological solution (300 ml) for 2.5 h, 70 h (about 3 days) and 286 h (about 12 days) and checking the chitosan release in solution.

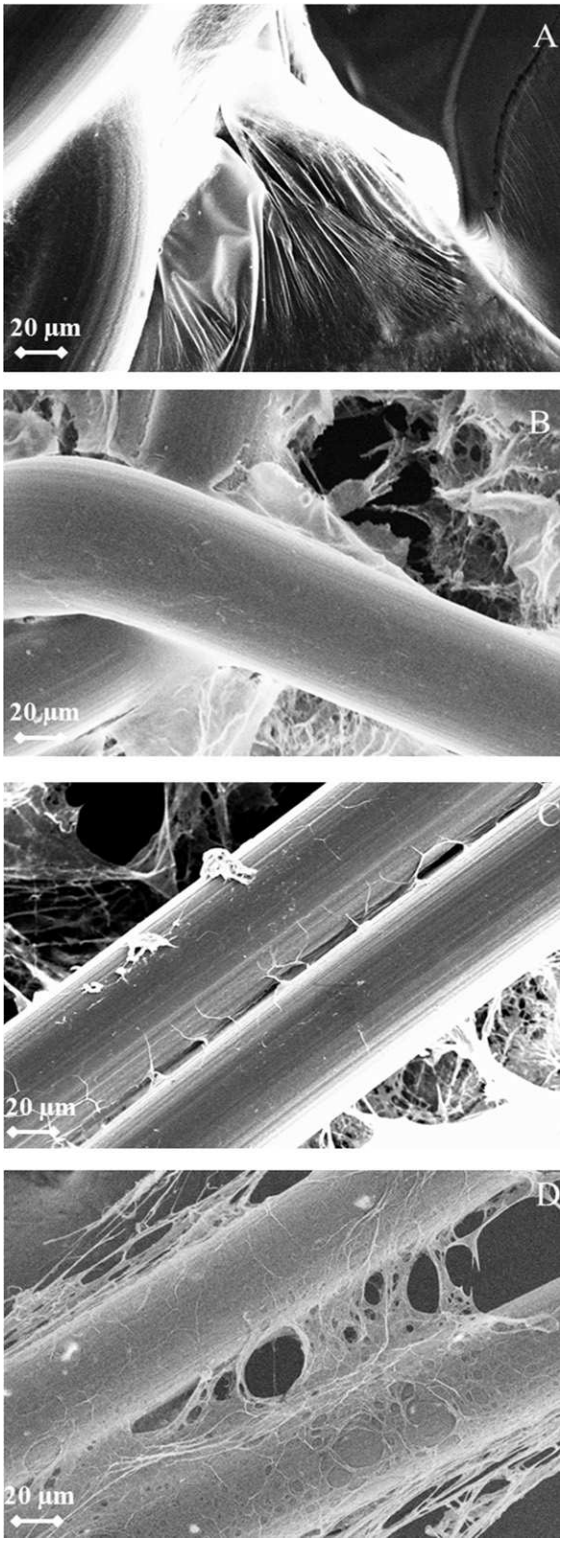

Fig. 8. SEM images of PP fibers functionalized with chitosan after 0 h (A), 2.5 h (B), 70 h (C) and 286 h (D) of immersion in physiological solution.

The evaluation of morphological modifications occurred after soaking was carried out by means of SEM-EDS analysis, the evaluation of chitosan amount released in solution was determined by means of the ninhydrin quantitative colorimetric determination [21].

SEM images are reported in Fig. 8. Immediately after the film deposition and after few hours of immersion (Fig. 8A and B,

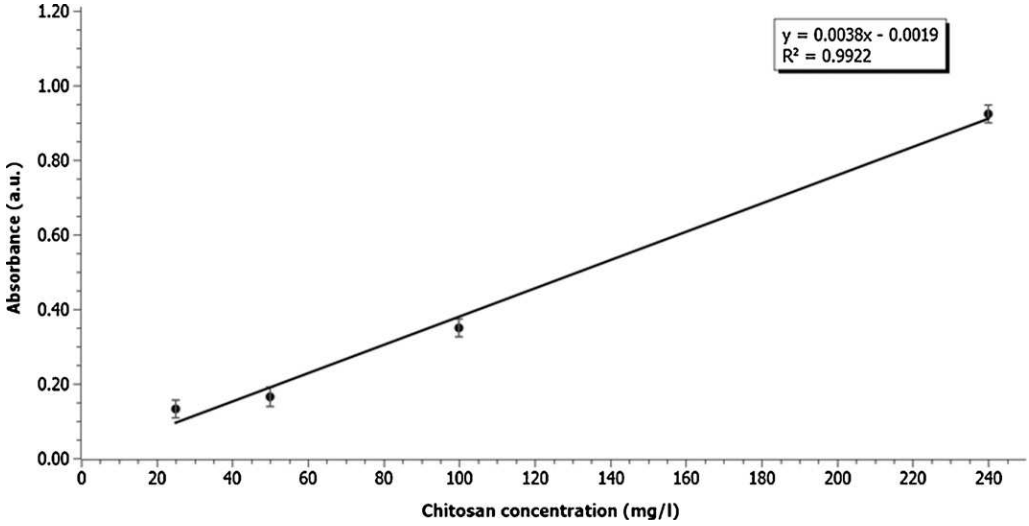

Fig. 9. Calibration curve chitosan-ninhydrin determined at 570 nm: absorbance shown as a function of chitosan concentration for the reaction chitosan–ninhydrin at pH 5.2 after 30 min of reaction time. Reliability of regressions: $R^2 > 0.99$.

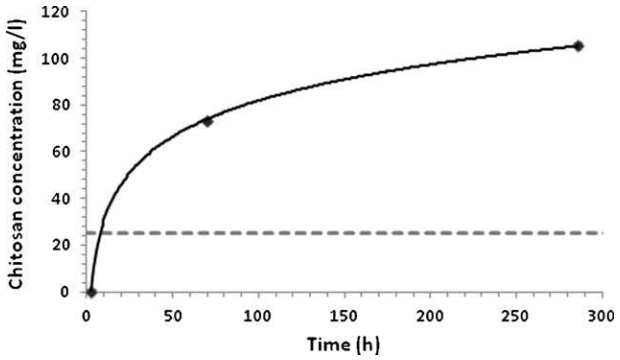

Fig. 10. Adhesion test: chitosan concentration released in physiological solution (extrapolated from the calibration curve reported in this figure shown as a function of soak time). The horizontal line indicates the detection limit (chitosan concentration < 25 mg/l).

respectively), chitosan film covers almost entirely PP fibers and the void space between the mesh network. After 3 days of immersion (Fig. 8C) the chitosan film degradation clearly appears and the empty space between the fibers are more visible. No further modifications are visible after 12 days of immersion (Fig. 8D).

The determination of chitosan released in physiologic solution is made up performing the Spackman colorimetric determination. The reaction involves the interaction between the primary amino group of chitosan with one ninhydrin molecule which leads to the formation of a compound that absorbs at 570 nm. The calibration curve is reported in Fig. 9 [21].

The trend of the release of chitosan in solution suggests a Michaelis–Menten-like kinetic (Fig. 10). The shape of the curve indicates that chitosan is almost completely released within the first 12 days of soaking.

4. Conclusions

PP mesh prosthesis, prepared through plasma activation, chitosan deposition and ethylene oxide sterilization, were characterized in terms of physico-chemical properties and chitosan release kinetics.

Both XRD and DSC techniques assessed the presence of a single crystalline isotactic phase for polypropylene fibers (α phase). Moreover, DSC allowed to evidence an increase of crystallinity degree of polypropylenic fibers due to plasma treatment.

Infrared spectroscopy showed the PP fibers surface oxidation as a consequence of plasma treatment, and the effective presence of chitosan after deposition procedure.

By TG analysis the chitosan thermal degradation was followed and a quantification of the chitosan amount deposited on PP fibers was obtained.

As for adhesion, results indicated that most of the chitosan was released in the first few days of soaking, and this is very positive for in vivo application since infections normally occur in the very first period after prosthesis implant.

Moreover, all the mesh preparation steps were observed via SEM/EDS techniques which allowed a direct view of the changes occurred in the samples morphology as a consequence of the treatments.

In conclusion, this physico-chemical approach makes possible to achieve an almost complete characterization of fibers during all their preparation steps.

This work was realized with the contribution of the European funding program POR-FESR ASSE I (I.1.3 Innovation and SME, Regione Piemonte) within the framework of the research project PREVI.

References

[1] P.K. Amid, A.G. Shulman, I.L. Lichtenstein, M. Hakakha, Biomaterials for abdominal wall hernia surgery and principles of their applications, Langenbecks Archiv fur Chirurgie 379 (1994) 168–171.
[2] C.R. Costello, S.L. Bachman, B.J. Ramshaw, S.A. Grant, Materials characterization of explanted polypropylene hernia meshes, Journal of Biomedical Materials Research Part B: Applied Biomaterials 83B (2007) 44–49.
[3] P. Bracco, V. Brunella, L. Trossarelli, A. Coda, F. Botta-Micca, Comparison of polypropylene and polyethylene terephthalate (Dacron) meshes for abdominal wall hernia repair: A chemical and morphological study Hernia 9 (2005) 51–55.
[4] A. Coda, F. Botta-Micca, A. Bona, C. Filippa, G. Ramellini, L. Attiè, G. Truda, Reperti istologici e alterazioni morfologiche delle protesi erniarie espiantate, Ospedali d'Italia Chirurgia 13 (2007) 64–72.
[5] R. D'Ambrosio, L. Capasso, S. Sgueglia, G. Iarrobino, S. Buonincontro, E. Carfora, E. Borsi, La protesi in polipropilene in chirurgia d'urgenza per laparoceli e ernie strozzate, Annali Italiani di Chirurgia LXXV (5) (2004) 569–573.
[6] C.B. Iglesia, D.E. Fenner, L. Brubaker, The use of mesh in gynecologic surgery, International Urogynecology Journal 8 (1997) 105–115.
[7] M.J. Cozad, D.A. Grant, S.L. Bachman, D.N. Grant, B.J. Ramshaw, S.A. Grant, Materials characterization of explanted polypropylene, polyethylene terephthalate, and expanded polytetrafluoroethylene composites: Spectral and thermal

analysis, Journal of Biomedical Materials Research Part B: Applied Biomaterials 94B (2010) 455–462.
[8] A. Coda, R. Lamberti, S. Martorana, Classification of prosthetics used in hernia repair based on weight and biomaterial, Hernia 16 (2012) 9–20.
[9] A. Rivaton, D. Lalande, J.L. Gardette, Influence of the structure on the (-irradiation of polypropylene and on the post-irradiation effects, Nuclear Instruments and Methods in Physics Research Section B: Beam Interactions with Materials and Atoms 222 (2004) 187–200.
[10] J. Lacoste, D. Vaillant, D.J. Carlsson, Gamma-, photo-, and thermal ly-initiated oxidation of isotactic polypropylene, Journal of Polymer Science Part B: Polymer Chemistry 31 (1993) 715–722.
[11] L. Costa, I. Carpentieri, P. Bracco, Post electron-beam irradiation oxidation of orthopaedic, UHMWPE Polymer Degradation and Stability 93 (2008) 1695–1703.
[12] C.K.S. Pillai, W. Paul, C.P. Sharma, Chitin and chitosan polymers: chemistry, solubility and fiber formation, Progress in Polymer Science 34 (2009) 641–678.
[13] M. Kong, X.G. Chen, K. Xing, H.J. Park, Antimicrobial properties of chitosan and mode of action: a state of the art review, International Journal of Food Microbiology 144 (2010) 51–63.
[14] J. Berger, M. Reist, J.M. Mayer, O. Felt, R. Gurny, Structure and interactions in chitosan hydrogels formed by complexation or aggregation for biomedical applications, European Journal of Pharmaceutics and Biopharmaceutics 57 (2004) 35–52.
[15] S.Y. Park, K.S. Marsh, J.W. Rhim, Characteristics of different molecular weight chitosan films affected by the type of organic solvents, Journal of Food Science 67 (2002) 194–197.
[16] Y.H. Lee, C.H. Yi, M.J. Chung, G.Y. Yeom, Characteristics of He/O_2 atmospheric pressure glow discharge and its dry etching properties of organic materials, Surface and Coatings Technology 146 (2001) 474–476.
[17] F. Arefi-Khonsari, J. Kurdi, M. Tatoulian, J. Amouroux, On plasma processing of polymers and the stability of the surface properties for enhanced adhesion to metals, Surface and Coatings Technology 142 (2001) 437–448.
[18] R. Dorai, M.J. Kushner, A model for plasma modification of polypropylene using atmospheric pressure discharges, Journal of Physics D: Applied Physics 36 (2003) 666–685.
[19] Y.I. Yun, J. Kurdi, K.S. Kim, S.J. Uhm, B.B. Khatua, K. Cho, J.K. Kim, C.E. Park, Aging behavior of oxygen plasma-treated polypropylene with different crystallinities, Journal of Adhesion Science and Technology 18 (2004) 1279–1291.
[20] S. Moore, Amino acid analysis: aqueous dimethyl sulfoxide as solvent for the ninhydrin reaction, Journal of Biological Chemistry 243 (1968) 6281–6283.
[21] S. Prochazkova, K.M. Vårum, K. Østgaard, Quantitative determination of chitosans by ninhydrin, Carbohydrate Polymers 38 (1999) 115–122.
[22] M. Rabiej, S. Rabiej, Analysis of synchrotron WAXD curves of semi-crystalline polymers by means of the Optifit computer program, Fibres and Textiles in Eastern Europe 13 (2005) 75–78.
[23] X. Li, H. Wu, Y. Huang, Y. Shi, Y. Wang, F. Xiang, Z. Zhou, β/α transformation of β-polypropylene during tensile deformation: effect of crystalline morphology, Colloid and Polymer Science 288 (2010) 1539–1549.
[24] A.B. Gil'man, L.A. Rishina, Structural transformations in the bulk of polypropylene upon plasma treatment, High Energy Chemistry 37 (2003) 291–296.
[25] X. Qu, A. Wirsén, A.C. Albertsson, Effect of lactic/glycolic acid side chains on the thermal degradation kinetics of chitosan derivates, Polymer 41 (2000) 4841–4847.
[26] K. Ogawa, T. Yui, Crystallinity of partially N-acetylate chitosans, Bioscience, Biotechnology, and Biochemistry 57 (9) (1993) 1466–1469.
[27] D.G. Dikobe, A.S. Luyt, Morphology and properties of polypropylene/ethylene vinyl acetate copolymer/wood powder blends composites, Express Polymer Letters 3 (2009) 190–199.
[28] S.K. Liao, C.C. Hung, M.F. Lin, A kinetic study of thermal degradations of chitosan/polycaprolacta blends, Macromolecular Research 12 (5) (2004) 466–473.
[29] Y. Dong, Y. Ruan, H. Wang, Y. Zhao, D. Bi, Studies on glass transition temperature of chitosan with four techniques, Journal of Applied Polymer Science 93 (4) (2004) 1553–1558.
[30] J.B. Gonzáles-Campos, E. Prokhorov, G. Luna-Bárcenas, A. Fonseca-García, I.C. Sanchez, Dielectric relaxations of chitosan: the effect of water on the α-relaxation and the glass transition temperature, Journal of Polymer Science Part B: Polymer Physics 47 (22) (2009) 2259–2271.